

## Supplemental material

Kiser et al., <https://doi.org/10.1085/jgp.201711815>

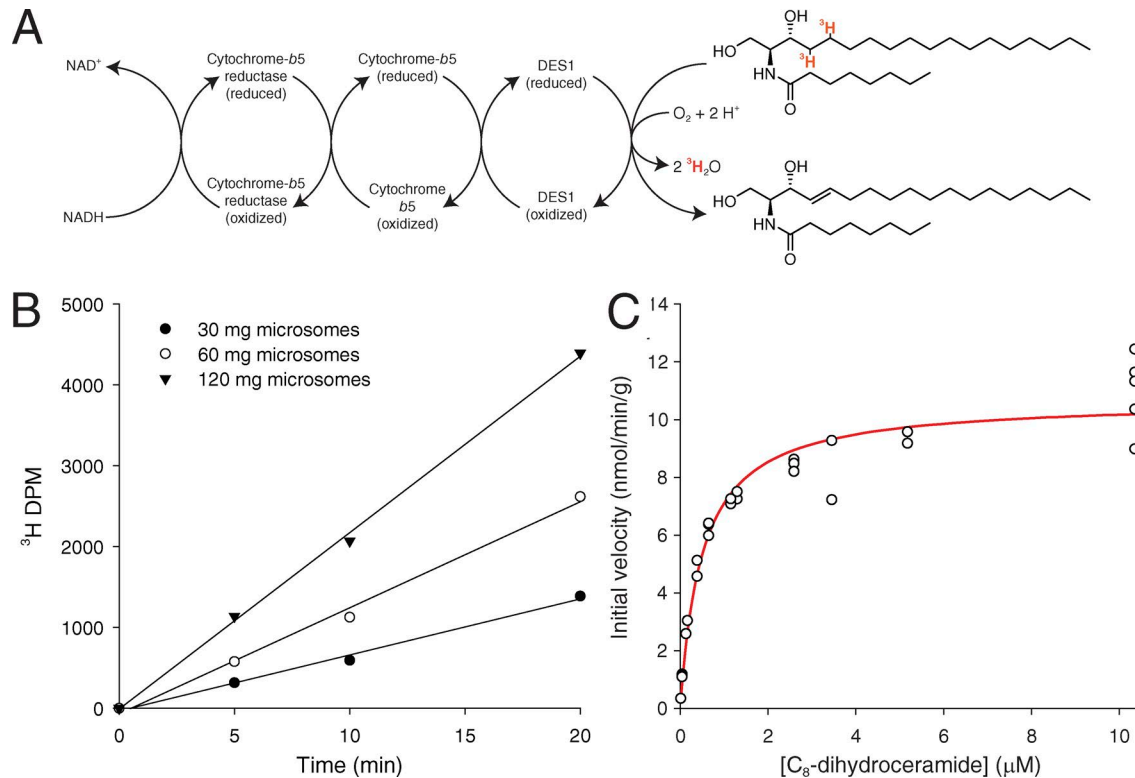


Figure S1. **Schematic and validation of the DES1 activity assay.** (A) DES1 dihydroceramide desaturase activity relies on NADH to provide electrons needed for production of an electrophilic, activated oxygen species that abstracts hydrogen from the substrate. The assay system uses a <sup>3</sup>H-4,5-labeled synthetic dihydroceramide as a substrate. DES1 activity specifically releases tritium from the substrate as water, which is separated from unreacted substrate and measured to quantify enzymatic activity. (B) Assessment of the linear range of the DES1 activity assay. Reactions were performed at 37°C for 0, 5, 10, and 20 min in the presence of 30, 60, and 120 mg *Lrat*<sup>-/-</sup> mouse liver microsomes at a fixed substrate concentration of 0.5 μM. Under these conditions, the assay was relatively linear with respect to both time and enzyme concentration. (C) Steady-state kinetics of mouse liver DES1 activity toward C<sub>8</sub>-dihydroceramide. Assays were performed as described in the Materials and methods section with increasing concentrations of unlabeled C<sub>8</sub>-dihydroceramide and a fixed quantity of 4,5-<sup>3</sup>H-C<sub>8</sub>-dihydroceramide.  $V_{max}$  and  $K_m$  values of  $10.7 \pm 0.3$  nmol/min/g and  $0.50 \pm 0.07$  μM, respectively, were determined for this assay system based on a total number of 28 data points measured in three separate experiments spanning a range of C<sub>8</sub>-dihydroceramide concentrations from 0.011 to 10.4 μM.

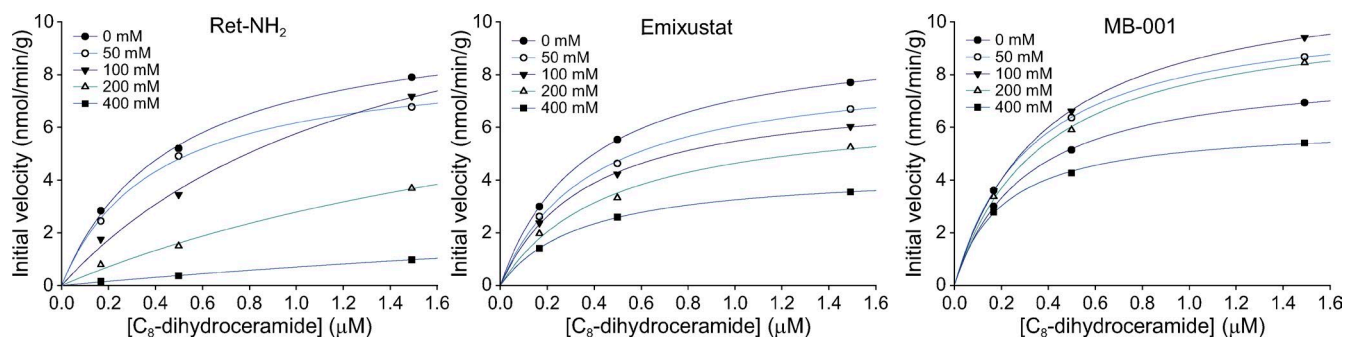


Figure S2. **Effects of RPE65 inhibitors on DES1 enzymatic function.** DES1 dihydroceramide desaturase assays were performed according to the standard method in the presence of the indicated compounds at substrate concentrations below, at, and above the  $K_m$  value for C<sub>8</sub>-dihydroceramide. The steady-state kinetic constants and the best fit mode of reversible inhibition derived from global curve fitting along with the estimated  $K_i$  values are shown in Table S1.

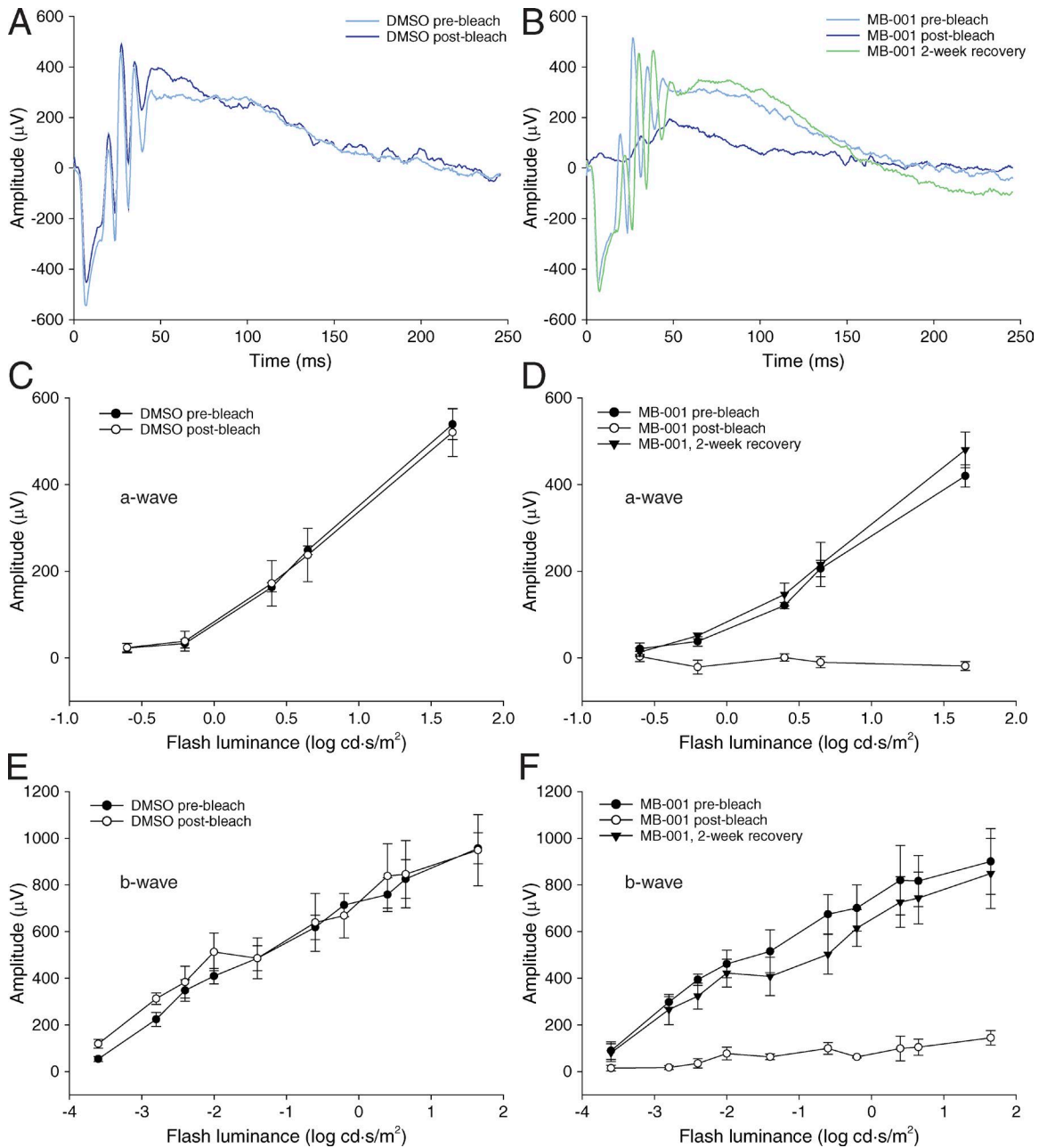


Figure S3. **Effects of MB-001 on dark-adapted mouse ERG responses.** (A and B) ERG responses to a 1.65 log cd-s/m<sup>2</sup> strobe flash recorded from mice (C57BL/6J, 2 mo old) that received IP DMSO vehicle or 8 mg/kg MB-001 immediately before, 22 h after, and 2 wk after a strong photobleach (10 min × 10,000 lux). (C and D) Plots of the scotopic a-wave amplitudes for the two groups of mice. (E and F) Scotopic b-wave amplitudes for the two groups of mice. DMSO group, *n* = 4; MB-001 group, *n* = 3. The data are shown as means ± SEM.

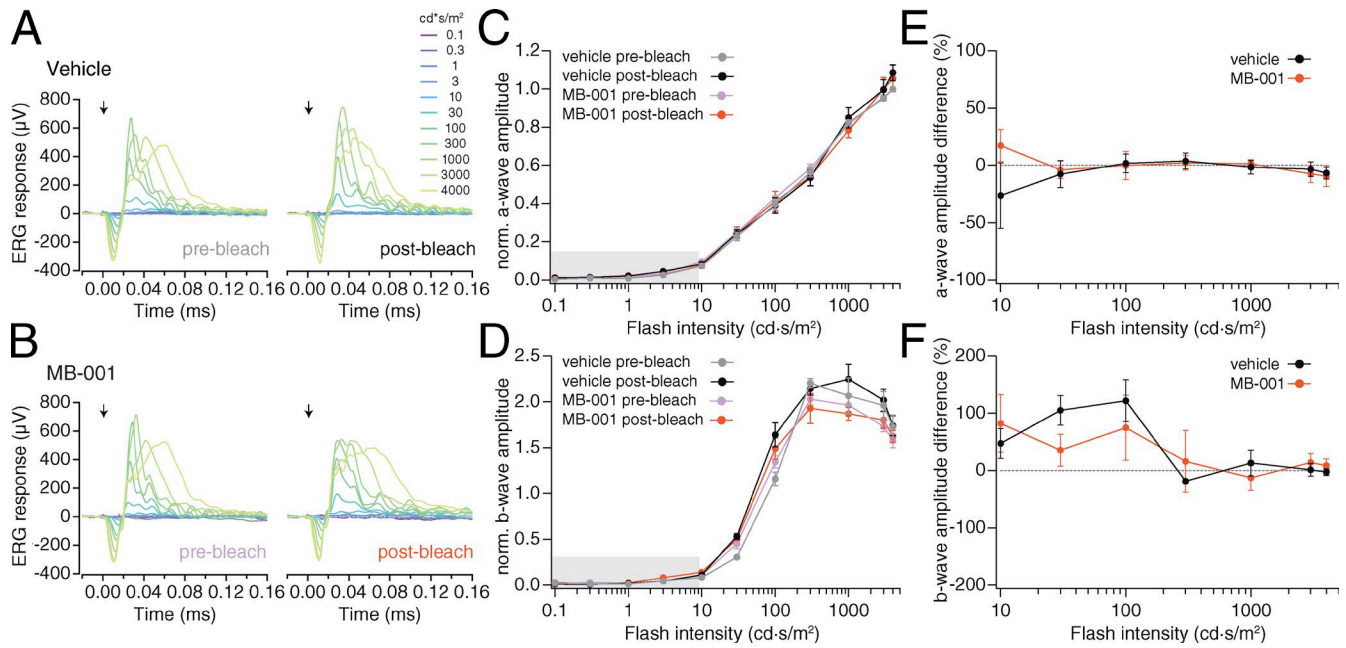


Figure S4. **Impact of MB-001 treatment on ERG responses in ground squirrels after the multiday dosing schedule used in wild-type mice. (A and B)** ERG responses from a single representative ground squirrel after vehicle (A) or MB-001 (B) treatment showing minimal effects of MB-001 treatment on cone function. ERG recordings were made in light-adapted 6-mo-old squirrels after 3 d of vehicle or MB-001 treatment before (left) and 10 min after (right) bleaching (see Materials and methods) using a brief flash of variable intensity as stimulation (black arrows, three to five trials per flash intensity). During the 3 d of treatment, animals were housed in normal cyclical lighting conditions. **(C and D)** Treatment group averages of ERG responses, which do not reveal systematic differences between vehicle- and MB-001-treated animals. We obtained mean a-wave and b-wave amplitudes at each light intensity after normalization by the a-wave amplitude to the 4,000 cd-s/m<sup>2</sup> flash before bleaching. We excluded responses to flash intensities <10 cd-s/m<sup>2</sup> (shaded regions) because they were small and corrupted by noise. **(E and F)** Changes in ERG responses induced by bleaching are not significantly different between treatment groups using this original treatment schedule. We obtained mean a-wave and b-wave amplitude differences (prebleach response - postbleach response; *n* = 4 squirrels; error bars represent SEM) that show no significant differences at any light intensity between treatments. We compared these ratios as paired measurements (vehicle vs. MB-001) with Wilcoxon rank-sum tests using 5% as the significance level.

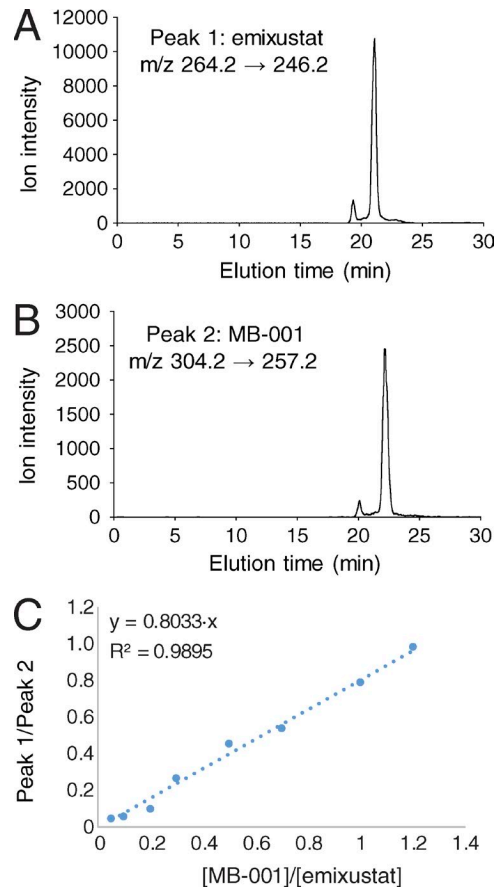


Figure S5. **Standard curve for MB-001 quantification.** 2 nmol emixustat was spiked into a serial solution of MB-001 (0–2.4 nmol) in ethanol. 100  $\mu$ l of the resulting solutions was injected into a liquid chromatography/mass spectrometry system. **(A and B)** The peak areas of emixustat chromatograms, recorded by selective reaction monitoring at m/z 264.2→246.2 (A) and MB-001 at m/z 304.2→257.2 (B), were recorded. **(C)** A standard curve depicting the ratio of the corresponding peak areas of MB-001 to emixustat and the ratio of their known amounts used in the experiment.

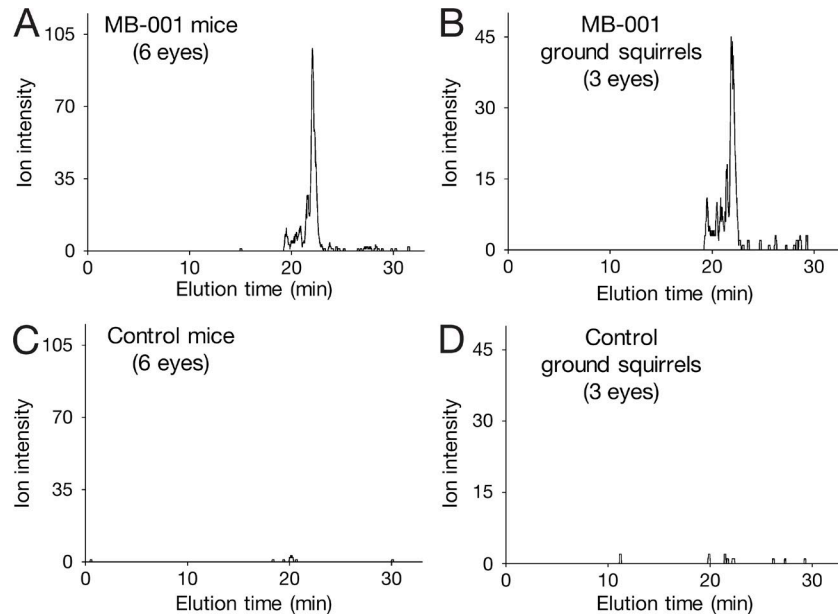


Figure S6. **Quantification of MB-001 levels in mouse and squirrel eyes.** Eye extracts were dissolved in ethanol containing 2 nmol emixustat. 100  $\mu$ l of the solution was injected into the liquid chromatography/mass spectrometry system. **(A–D)** The chromatogram obtained by selective reaction monitoring at  $m/z$  304.2 $\rightarrow$ 257.2 demonstrated that the eyes of C57BL/6J mice (A) and ground squirrels (B) treated with MB-001 both contained substantial amounts of the compound, although the peaks of MB-001 in the eyes from the animals treated with DMSO were negligible (C and D). The amounts of MB-001 in both animals were calculated based on the standard curve shown in Fig. S5.

Table S1. **Steady-state kinetic constants obtained for DES1-mediated dihydroceramide desaturase activity in the presence of RPE65 inhibitors**

Concentration	Emixustat		MB-001		Ret-NH <sub>2</sub>	
	$V_{max}$	$K_m$	$V_{max}$	$K_m$	$V_{max}$	$K_m$
$\mu$ M						
400	4.4	0.35	6.1	0.21	4.9	6.1
200	6.8	0.47	10.5	0.37	10.4	2.7
100	7.5	0.37	11.9	0.39	13.9	1.4
50	8.4	0.38	10.6	0.33	8.6	0.40
0	9.6	0.37	8.3	0.30	10.3	0.47
Mode of inhibition	Noncompetitive; $K_i = 360 \mu$ M		Noninhibitory		Partial mixed or uncompetitive; $K_i = \sim 80 \mu$ M	

$V_{max}$  and  $K_m$  values were derived by curve fitting as shown in Fig. S2. The bottom row shows the best fit mode of inhibition and associated  $K_i$  values derived from global analysis of the data. The activity simulation and minor inhibition of DES1 activity at higher concentrations precluded global fit analysis for MB-001.